

Transient Behavior of Aerosol Filtration in Model Filters

The transient behavior of aerosol filtration in model filters composed of several layers of wire screens was investigated experimentally. The collection efficiency of the filter expressed in terms of the single fiber efficiency was determined under a variety of conditions. The increase in the collection efficiency and pressure drop during the course of filtration was examined. An empirical correlation relating the increase of the collection efficiency as a function of the amount of deposition was established.

H. EMI, CHIU-SEN WANG and
CHI TIEN

Department of Chemical Engineering and
Materials Science
Syracuse University, Syracuse, NY 13210

SCOPE

This study was undertaken in order to obtain experimental results pertaining to the transient behavior of aerosol filtration in fibrous model filters. Although fibrous filtration is a transient process by nature, most of the research work carried out in this area is concerned primarily with the initial period of filtration during which the effect of deposited aerosol particles can be neglected. It is obvious that a rational design of fibrous filtration cannot be made with results obtained from the consideration of the initial period of filtration alone.

The retention of particles within a fibrous filter results in an accumulation of particles at the surface of the packing fibers. The effect is manifested mainly in two ways; the deposited particles act as additional collectors thereby increasing the collection efficiency of the filter; at the same time, as the filter becomes increasingly clogged, the pressure drop necessary to maintain a given flow rate through the filter increases. The termination of operation of a fibrous filter is often dictated by

excessive pressure drop increase.

The principal objective of this work is to study experimentally the change of the collection efficiency and pressure drop of fibrous model filters beginning with clean filters to the stage where the filter becomes nearly clogged. The model filters were composed of layers of wire screens of different dimensions. The experiments were conducted under conditions such that the inertial impaction was the dominant mechanism for particle collection.

The purpose of using model filters for the experimental work was two-fold. First, model filters provide a more defined structure to facilitate the interpretation of data. Second, the model filters composed of wire screens lend themselves to filter cleaning and therefore offer certain potential advantages. It is likely that practical devices, based on model filter structure, can be developed in the future.

CONCLUSIONS AND SIGNIFICANCE

The transient behavior of aerosol filtration in fibrous model filters was studied experimentally. The results of this work yield the following information: (a) pressure drop across the filter in its clean state; (b) the initial collection efficiency of the filter expressed as the single fiber collection efficiency; (c) the change of the collection efficiency; and (d) the increase in pressure drop across the filter as the filter becomes increasingly clogged. Both the change of the collection efficiency and the increase in the pressure drop were found to be very significant, by more than one order of magnitude over the initial value.

The experimental results indicate that the collection efficiency increases monotonically with the increase in particle deposition at low gas velocities. At high gas velocity, the collection efficiency first increases with the increase in deposition, reaching a maximum, the collection efficiency remains at this value or even suffers a slight decrease with further increase in deposition, suggesting the effect of particle reentrainment and/or particle bounce-off. On the other hand, the pressure drop was found to increase monotonically with the amount of particle deposition for all gas velocities.

Based on the data collected in this study, empirical correlations relating the change in collection efficiency with the amount of particle deposition as well as other variables were successfully established. Less accurate correlations relating the increase in pressure drop with the amount of deposition were

also obtained. These correlations can be used to predict the transient dynamic behavior of model filters composed of layers of wire screens.

Although fibrous filtration has been a topic of extensive study during the past two decades, these studies are largely confined to the initial stage of filtration. For example, in the experimental determination of the collection efficiency, the overwhelming majority of the effort has been expended toward the study of clean filters. Similarly, most of the theoretical work, both in the prediction of pressure drop and collection efficiency, employs models which are not capable of incorporating the effect of particle deposition on filter performance. Consequently the results of these investigations have made only minimum impact on the engineering practice of fibrous filtration, a fact which has been pointed out by the critics of aerosol filtration research (Dyment, 1978) as well as readily conceded by workers in the field (Davies, 1973).

The main features of the dynamic behavior of fibrous filtration are the histories of the effluent concentration and the pressure drop necessary to maintain the operation. Since fibrous filtration is inherently time-dependent, the knowledge of the transient dynamic behavior of fibrous filters is necessary before any rational design can be contemplated. The basic information of primary importance in this regard are:

- (1) The change of the collection efficiency of the filter element as a function of deposition.
- (2) The effect of particle deposition on the media structure as manifested by the flow-rate pressure drop relationship.

The present investigation is concerned with the study of the

H. Emi is presently with the Department of Chemical Engineering, Kanazawa University Kanazawa, Japan.
0001-1541-82-5580-0397-42.00. © The American Institute of Chemical Engineers, 1982.

transient behavior of model filters composed of a large number of wire screens of various dimensions. The use of model filters in aerosol research was pioneered by Fuchs and his coworkers some time ago (Fuchs and Stechkina, 1963). However, its use has been limited to the investigation of the initial stage of filtration. The advantage of model filters is, of course, their known ge-

ometry which permits more rigorous analysis and avoids the uncertainty encountered in real filters. Another potential advantage of wire screen model filters is their relative rigidity allowing periodical cleaning of filter elements as the dust load becomes heavy. This is an important consideration since filters capable of renewal can be used repetitively.

EXPERIMENTAL APPARATUS, METHOD AND PROCEDURES

A schematic diagram of the apparatus used for the measurements is shown in Figure 1. The main functions of the apparatus are:

- (1) To generate monodispersed aerosol streams with reasonably high particle concentrations at a volumetric flow rate of up to 100 L/min.
- (2) To determine the collection efficiency of model filters composed of layers of wire screens over long periods of operation until nearly complete clogging is achieved.
- (3) To measure the pressure drop increase during filtration runs.

Aerosol Generation

The aerosol generator used in this work was based on the original design of Whipple (1972) and is similar to the one described by Liu et al. (1966). Test aerosols were prepared by first dispersing a stearic acid-ethanol solution into polydispersed droplets with the use of a collision atomizer. The polydispersed aerosol was passed into a pyrex tube composed of two sections: a heating section, followed by a condensing section. In the heating section, the droplets were vaporized and reduced to nuclei. In the condensing section, monodispersed stearic acid aerosols were formed by the condensation of stearic acid vapor on the nuclei. The aerosol suspension was

further diluted to give the desired concentration for experiments.

Test Section

The test section consists of an aerosol tunnel (6 in. diameter) followed by a contraction tunnel. The diameter of the contraction tunnel varies from 6 in. at the upper end to 1.5 in. at the lower end. The purpose of the contraction tunnel is to produce a uniform aerosol flow leading to the model filter. The contraction tunnel was made by applying layers of epoxy resin and fiberglass to a smooth waxed wooden pattern.

The construction of the model filters is as follows: Filter elements composed of layers of wire screens (up to sixteen layers) are held together between two flanges with three springs. Each piece of screen is attached to an aluminum ring [i.d. 1.5 in.; o.d. 2.5 in. with 1 mm thickness]. When a multilayer screen element is assembled, extra aluminum rings are placed between the screen as spaces. Rubber cement is applied on the sides of the element to eliminate air leakage. The specifications of the wire screens are given in Table 1.

Particle Concentration and Size Determination

For the calculation of the collection efficiency, the influent and effluent aerosol particle concentrations are required. The

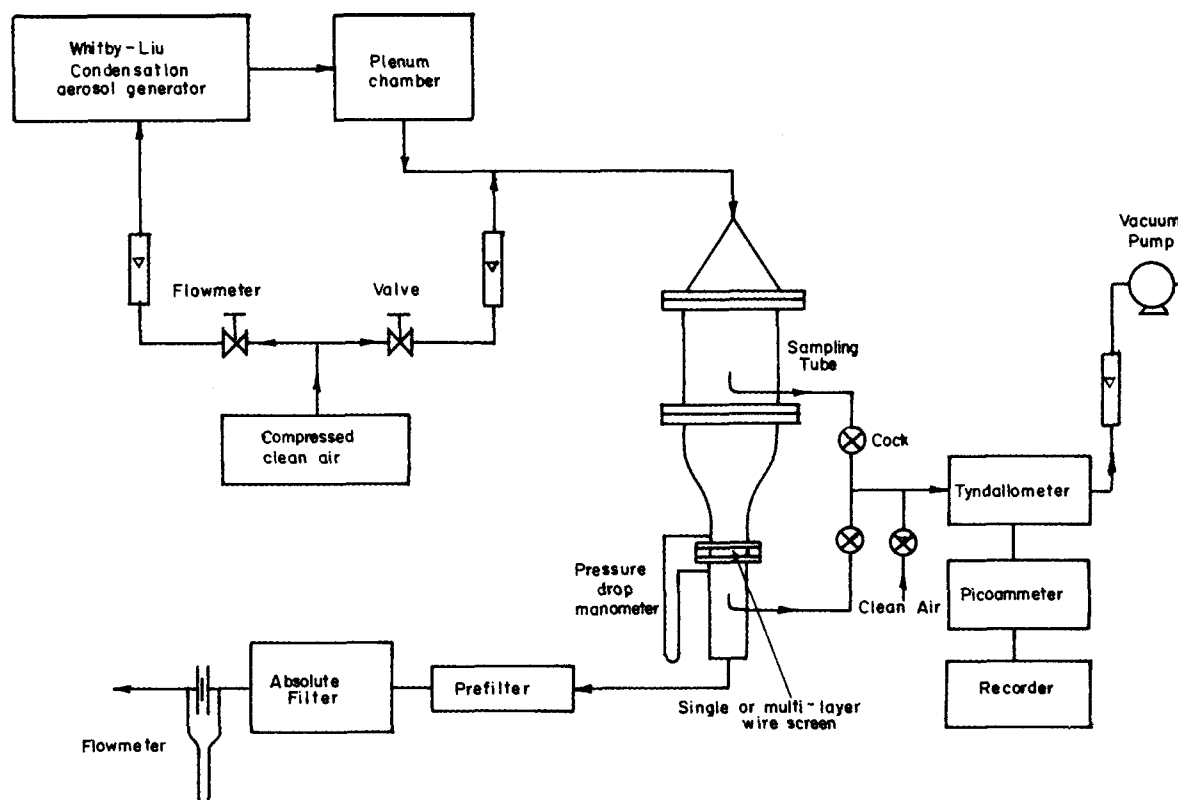


Figure 1. Schematic diagram of experimental apparatus.

TABLE 1. SPECIFICATIONS OF WIRE SCREENS (MEASURED BY OPTICAL MICROSCOPES)

Mesh	$2a_c$ [μm]	\bar{W}^* [μm]	$2h$ [μm]	$\left(\frac{\bar{W}}{2h}\right)^2 \times 100$ [%]	$(a_c/h) \times 100$ [%]
200	52.7	79.7	132	36.5	39.9
325	35.9	40.3	76.2	28.0	47.1
500	25.0	24.5	49.5	24.5	50.5

* \bar{W} : clearance between wires, $\bar{W} = 2h - 2a_c$.

Tyndallometer used in this work for the determination of aerosol particle concentration was constructed by Whipple (1972) based on the original design of Muir and Davies (1967).

The Tyndallometer readings provide a relative measurement of particle concentrations which is sufficient for the calculation of the collection efficiency. On the other hand, absolute particle concentrations are also needed in order to relate the transient behavior of the model filters with the extent of particle deposition (dust loading). For this purpose, membrane filters were used to determine the total concentration (wt. of particle per unit volume) by periodically sampling the influent aerosol stream.

The aerosol particle size was determined by depositing the aerosol particles on a glass slide placed in an electrostatic sampler (Thermo-Systems Inc., Model 3100, St. Paul, Minnesota) and examining them under a microscope.

EXPERIMENTAL RESULTS

A large number of experimental runs were made using model filters composed of different layers of wire screens. All the experiments were performed under constant flow rate conditions. The experimental conditions are summarized as follows:

Properties of Aerosol Particles

Particle Substance	Stearic acid
Particle Density	$\rho_p = 0.94 \text{ g/cm}^3$
Particle Diameter	$d_p = 1.1 \mu\text{m}$
Particle Concentration (Influent)	$3.5 \sim 125 \text{ mg/m}^3$

Model Filters

Screen Wire	500, 325, 200 mesh
Wire Dimension	see Table 1
Cross section area	11.3 cm^2 (diameter 3.8 cm)
Number of Screen Layers	1 ~ 16
Distance Between Successive Screens	2 mm

Operating Conditions

Volumetric Flow rate	$3.1 \sim 78 \text{ L/min}$
Superficial Velocity	$4 \sim 115 \text{ cm/s}$
Stokes Number, N_{St}	5.65×10^{-3} to 3.07×10^{-1}
Reynolds Number (Based on Wire Diameter), N_{Re}	7.37×10^{-2} to 4.04

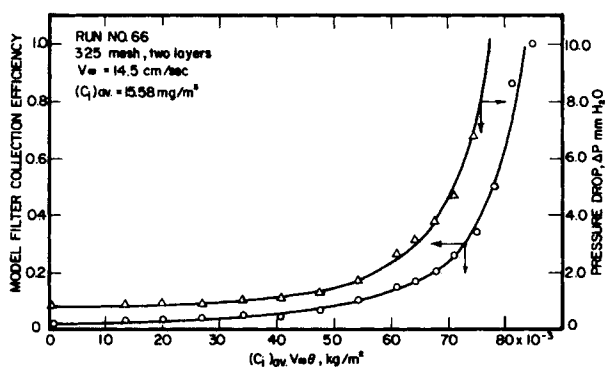


Figure 2. Typical set of model filter measurements.

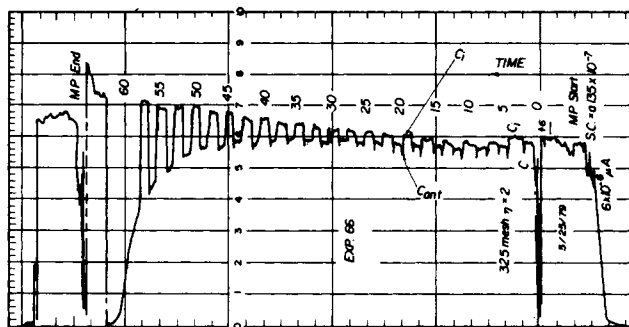


Figure 3. Tyndallometer readings of influent and effluent concentrations.

Relative Size Parameter, N_R	0.019 ~ 0.04
Peclet Number	$4 \times 10^4 \sim 2.19 \times 10^6$
Time Duration	up to 1 h

A typical set of measurement data is shown in Figure 2. The influent and effluent particle concentrations were based on Tyndallometer readings (Figure 3). In carrying out the filtration experiments, the influent and effluent streams were passed through the Tyndallometer alternatively for approximately five-minute duration (which was sufficient to overcome the transient effect). The readings corresponding to these discrete time intervals for either stream were then connected together to give continuous curve of concentration vs. time. The reported absolute particle concentration of the influent stream was based on the average value of the results of several sample analyses using millipore filters. The particle size was obtained from microscopic examination. The pressure drop data were obtained from manometers directly.

The Tyndallometer readings (Figure 3) have an accuracy of 1% of the full range. Thus it is difficult to measure the initial collection efficiency accurately. This was overcome by using a large number of screen layers so that a significant concentration change could be effected. The reliability and the reproducibility of the results are shown in Figure 4 (for collection efficiency) and Figure 5 (for pressure drop). In these figures, the abscissa variable is taken to be $(c_{in})_{av} V_{av} \theta$ instead of time θ . For a given filtration run, the influent aerosol particle concentration inevitably increases with time. This is due to the steady increase in the stearic acid concentration of the ethanol solution present in the collision atomizer since ethanol is more volatile than stearic acid. The variation in aerosol concentration ranged from 10 to 20% from its initial value. The use of $(c_{in})_{av} V_{av} \theta$ eliminates the need to consider the possible effect due to this difference in concentration. The reproducibility, on the average, is quite good as seen from these figures.

The consistency of the measurements can be seen by comparing the results obtained with model filters composed of different layers of wire screens. These are shown in Figure 6 (collection efficiency) and Figure 7 (pressure drop). The curves on these figures are orderly placed and conform to the fact that filters composed of a greater number of screen layers should give greater collection efficiency and greater pressure drop. Considering the inherent complexities of aerosol filtration measurements, the accuracy and consistency of the data must be judged to be satisfactory.

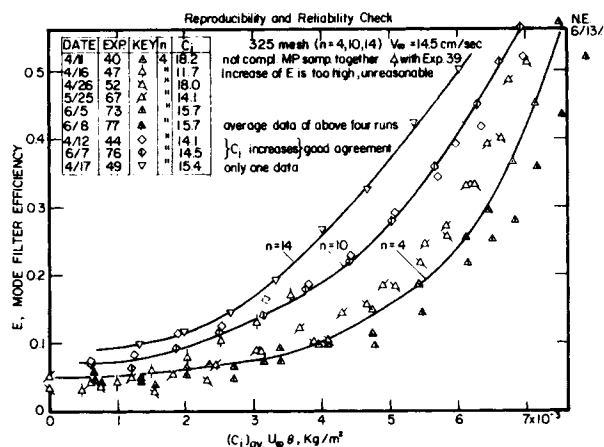


Figure 4. Reproducibility and reliability of experimental data.

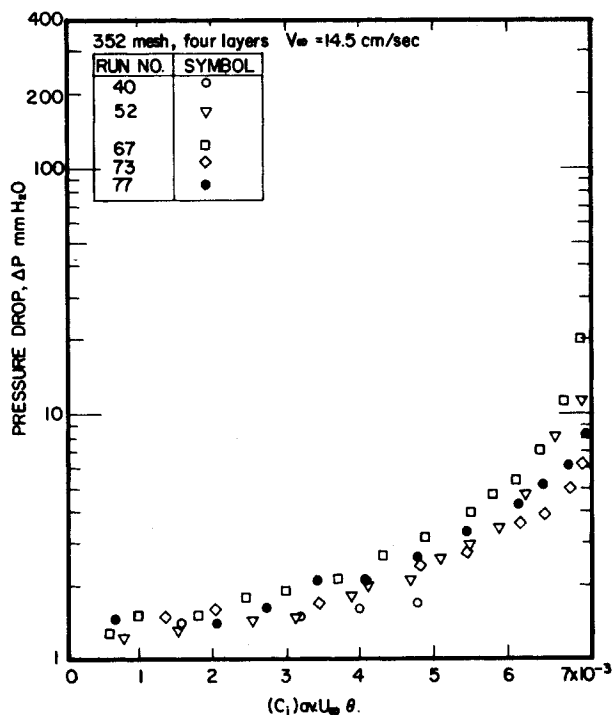


Figure 5. Consistency of pressure drop measurements.

INTERPRETATION OF RESULTS

The experimental data of particle collection were interpreted by the parallel fiber model. Thus each layer of the wire screen can be viewed as a composite of two layers of parallel fibers placed at right angles to each other. The collection efficiency of a single wire screen layer E_j and the single fiber efficiency of the wires constituting the screen, η_j are related by the expression (Tsiang, 1980)

$$1 - E_j = \left[1 - \eta_j \frac{a_c}{h} \right]^2 \quad (1)$$

On the other hand the total collection efficiency of a model filter composed of n layers of wire screens, E_t , can be expressed in terms of the collection efficiencies of the individual screen layer, E_j as follows

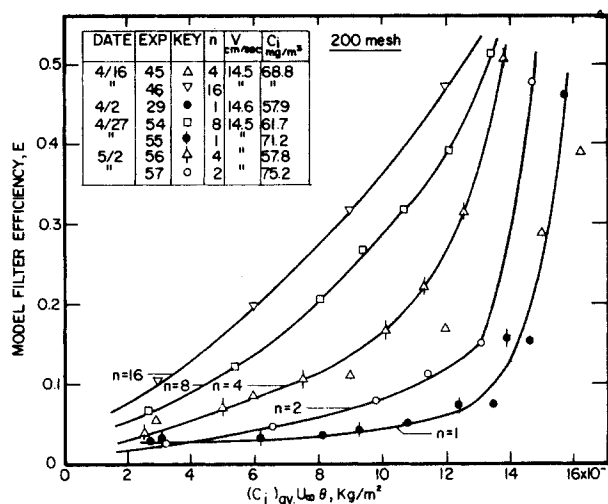


Figure 7. Consistency of experimental data as shown from multilayer model filter results.

$$1 - E_t = (1 - E_1)(1 - E_2) \dots (1 - E_n) = \prod_{k=1}^n (1 - E_k) \quad (2)$$

Also, by definition, one has

$$E_t = \frac{C_{in} - C_{eff}}{C_{in}} = 1 - \frac{C_{eff}}{C_{in}} \quad (3)$$

where C_{in} and C_{eff} are the particle concentrations of the influent and effluent streams respectively.

Combining Eqs. 1, 2 and 3, one has

$$\frac{C_{eff}}{C_{in}} = \prod_{k=1}^n \left(1 - \frac{a_c}{h} \eta_k \right)^2 \quad (4)$$

Initially the entire filter is clean, the single fiber efficiency of all the layers are the same and equal to the clean fiber efficiency, η_o . Equation 4 becomes

$$\frac{C_{eff}}{C_{in}} = \left(1 - \frac{a_c}{h} \eta_o \right)^{2n} \quad (5)$$

and

$$\eta_o = \frac{h}{a_c} \left[1 - \left(\frac{C_{eff}}{C_{in}} \right)^{1/2n} \right] \quad (6)$$

Equations 4 and 6 provide the basis for the interpretation of the model filter data. This will be explained in later sections.

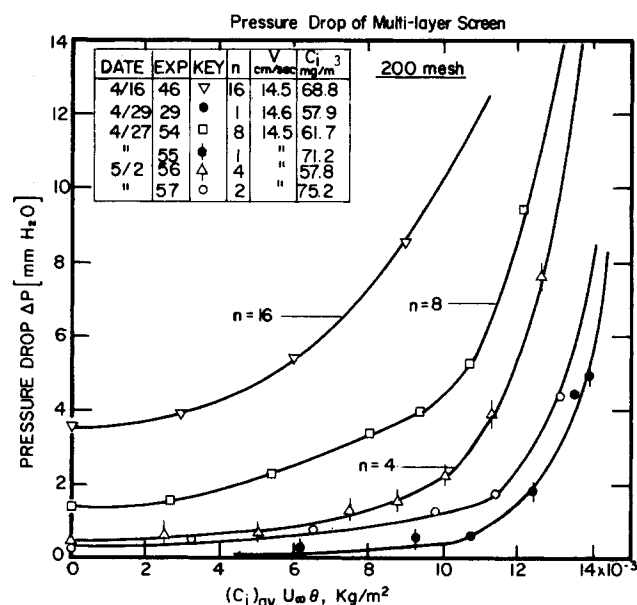


Figure 6. Consistency of experimental data as shown from multilayer model filter results (pressure drop).

Initial Pressure Drop

Most of the pressure drop data were obtained from measurements using model filters composed of ten layers of wire screens. The single layer pressure drop was obtained by dividing the total pressure drop by the number of screen layers. The conventional method of correlating pressure drop data was used. The drag coefficient, C_D , defined as

$$C_D = \frac{\Delta P / \frac{1}{2} \rho V_\infty^2}{\quad} \quad (7)$$

was calculated from the data and plotted against the Reynolds number, N_{Re} , defined as

$$N_{Re} = \frac{\rho V_\infty (2a_c)}{\mu} \quad (8)$$

as shown in Figure 8. Also included in this figure are the data reported earlier by Gentry and Choudhary (1975). A single straight line (on the log-log scale) namely

$$C_D = \frac{100}{N_{Re}} \quad (9)$$

is found to approximate the data reasonably well for N_{Re} up to 5 for all the screens covering a_c/h from 0.399 to 0.505.

Attempts were made to establish a more general correlation for

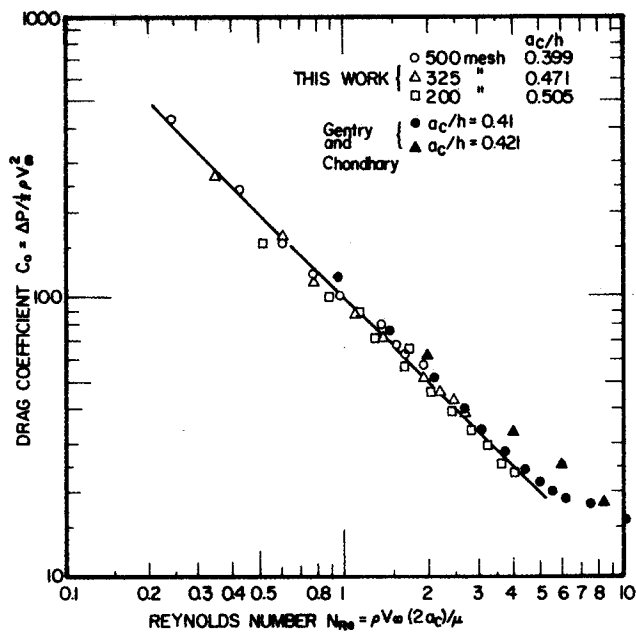


Figure 8. Drag coefficient of wire screen.

the prediction of pressure drop across wire screens with square openings. A simple dimensional analysis suggests that C_D should be a function of both the Reynolds number, N_{Re} and the ratio a_c/h or

$$C_D = C_D(N_{Re}, a_c/h) \quad (10)$$

If one assumes that a wire screen can be considered as the composite of two identical layers of parallel-fibers (with equal interfiber distance) placed at right angles, the drag force acting on the wire can be found from Miyagi's solution (1966) for the flow field around an array of equally placed parallel cylinders. The drag force acting on a unit length of wire is given as (Tsiang, 1980)

$$F_D = 8\pi\mu V_\infty a_0 \quad (11)$$

$$a_0 = \frac{1}{1 - 2 \ln(2t) + \frac{2}{3}t^2 \dots} \quad (12)$$

$$t = \frac{\pi a_c}{2h} \quad (13)$$

The pressure drop across a layer of the wire screen can be considered as the sum of the drag forces acting on all the wire segments, or

$$(\Delta P) = (2) \left(\frac{1}{2h} \right) F_D = \frac{8\pi\mu V_\infty a_0}{h} \quad (14)$$

The above expression can be rewritten as

$$\left(\frac{\Delta P}{\frac{1}{2}\rho V_\infty^2} \right) \left(\frac{(2a_c)\rho V_\infty}{\mu} \right) = (C_D)(N_{Re}) = (64) \frac{t}{1 - 2 \ln(2t) + \frac{2}{3}t^2 \dots} \quad (15)$$

Thus, if the parallel-fiber geometry is a valid representation of wire screens, the drag coefficient, C_D , is directly proportional to the right hand side of Eq. 15, which accounts for the dependence of C_d on a_c/h . However, when a correlation of the form $C_d[1 - 2 \ln(2t) + \frac{2}{3}t^2 \dots]$ vs. N_{Re} was sought, the data did not converge into a single curve. It is obvious that the interactions among the cross wires in a wire screen cannot be accounted for by the use of Miyagi's solution in the estimation of pressure drop.

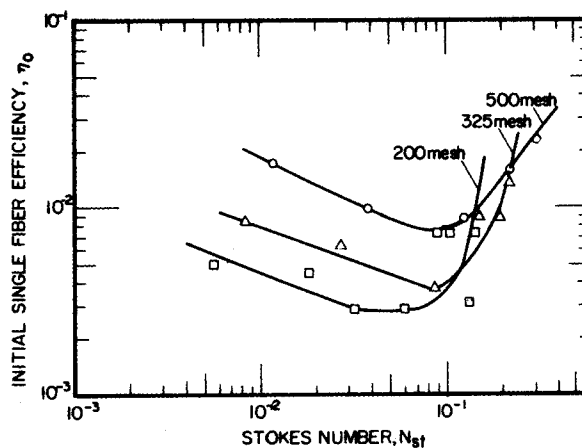


Figure 9. Single fiber collection efficiency of wire screen experimentally determined during initial stage.

Initial Collection Efficiency

As stated previously the initial collection efficiency of a single layer of wire screen is too low to be measured accurately. To overcome this difficulty model filters composed of ten layers of wire screens were used. The initial collection efficiency, E_0 , can be calculated from the influent and effluent concentrations, C_{in} and C_{eff} ; namely from Eq. 6, for $n = 10$

$$\eta_0 = \left(\frac{h}{a_c} \right) \left[1 - \left(\frac{C_{eff}}{C_{in}} \right)^{1/20} \right] \quad (16)$$

The experimental data are presented in the form η_0 vs. N_{St} the Stokes number as shown in Figure 9. The presence of a minimum in the $\eta_0 - N_{St}$ curve is characteristic of the situation in which the dominant mechanisms of collection are the Brownian diffusion and inertial impaction.

EFFECT OF DEPOSITION ON MODEL FILTER PERFORMANCE

The major part of this phase of the study is directed toward an understanding of the effect of particle deposition on filter performance, to obtain pertinent data, and if possible, to develop quantitative relationships between filter performance and the extent of deposition. Information such as this has rarely been reported before although its importance is generally recognized.

The complexities of the effect of deposition on filter performance can be seen from the data shown in Figures 10 and 11 in which the collection efficiency and pressure drop across a model filter consisting of a single layer of 200 mesh wire screens are shown

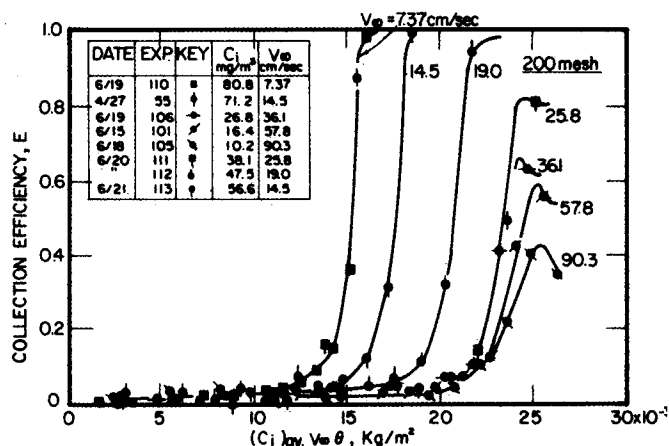


Figure 10. Change of collection efficiency with flow velocity.

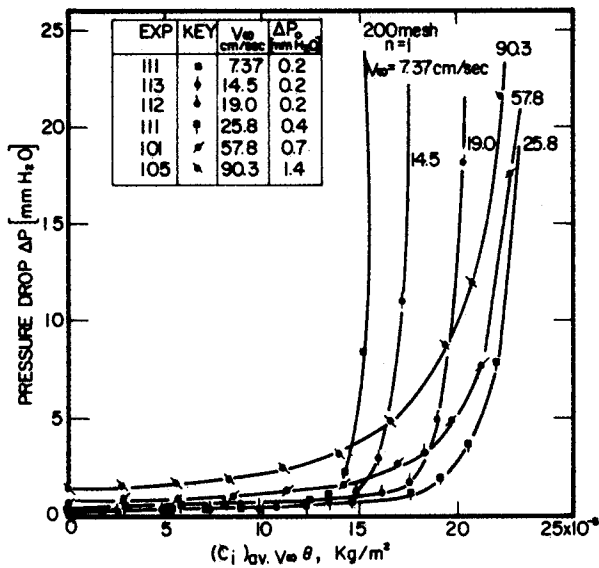


Figure 11. Increase in pressure drop at different air velocities.

as functions of $(C_{in})_{av} V_{\infty} \theta$. The collection efficiency is found to increase with time. This increase occurs sooner for lower gas velocity. For V_{∞} greater than 20 cm/s the maximum collection efficiency achieved was less than unity (i.e., no complete cake formation). Furthermore, at high gas velocities, the collection efficiency increases first, reaches a maximum value and then decreases, a phenomenon similar to that observed earlier (First and Hinds, 1976).

The pressure drop data exhibited similar but more complex behavior. The curves corresponding to different gas velocities (Figure 11) are not arranged in an orderly manner as in the case of the collection efficiency curves (Figure 10). This perhaps explains the relative difficulty encountered in correlating the pressure drop data to be explained later.

The experimental data obtained in this study are the influent and effluent particle concentrations and pressure drops of model filters composed of various layers of wire screens. To obtain the transient behavior of the model filters, and specifically the effect of particle deposition on filter performance, the following procedures were developed. First from Eq. 1, for the k -th layer of screen, one has

$$1 - E_k = \left(1 - \eta_k \frac{a_c}{h}\right)^2 = 1 - \frac{C_{k-1} - C_k}{C_{k-1}} = \frac{C_k}{C_{k-1}} \quad (17)$$

where C_k and C_{k-1} are the particle concentrations of the gas

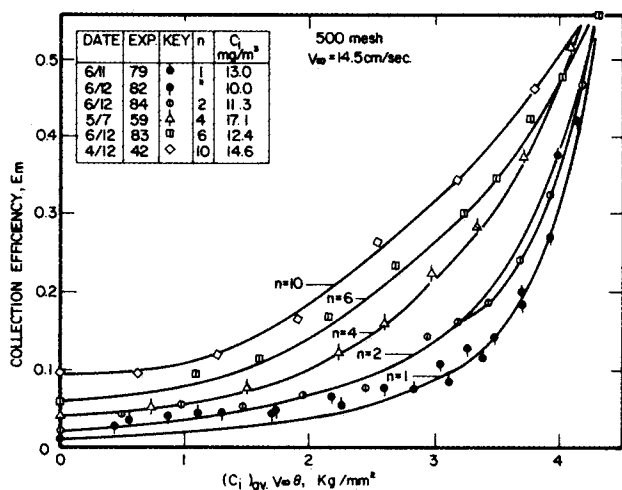


Figure 12. Efficiency of multi-layers model filters.

streams leaving the k -th and $(k-1)$ th layer respectively. By definition one has

$$C_k/C_{in} = 1 - (E_t)_k \quad (18.a)$$

$$C_{k-1}/C_{in} = 1 - (E_t)_{k-1} \quad (18.b)$$

where $(E_t)_k$ and $(E_t)_{k-1}$ are the total collection efficiencies of model filters composed of k -layers of screens and $(k-1)$ layers of screens respectively. Combining Eq. 17 with Eqs. 18.a and 18.b yields

$$\eta_k = \frac{h}{a_c} \left[1 - \sqrt{\frac{1 - (E_t)_k}{1 - (E_t)_{k-1}}} \right] \quad (19)$$

Namely one can obtain the single fiber collection efficiency of the k -th screen if the total collection efficiency of model filters composed of $(k-1)$ layers and that of k layers are known. Furthermore, the extent of deposition can be described by the amount of particles deposited per unit area of a given layer of screen, denoted by m_k . By a material balance, one has

$$(C_{k-1} - C_k)V_{\infty} = \frac{dm_k}{d\theta} \quad (20)$$

or

$$\begin{aligned} m_k &= \int_0^{C_{in} V_{\infty} \theta} \left(\frac{C_{k-1}}{C_{in}} - \frac{C_k}{C_{in}} \right) d(C_{in} V_{\infty} \theta) \\ &= \int_0^{C_{in} V_{\infty} \theta} [(E_t)_k - (E_t)_{k-1}] d(C_{in} V_{\infty} \theta) \end{aligned} \quad (21)$$

The area bound between the curve E vs. $C_{in} V_{\infty} \theta$ for model filters with $(k-1)$ layers of screens and the similar curve for the model filter with k layers of screen gives the value of m_k .

The equations presented above make it possible to evaluate the single fiber efficiency as a function of the amount of deposition from the model filter experimental data. In practice, the increment in the number of screen layers of the experimental model filters was not always one. For example, the 325 mesh model filter used had one, two, four, six, ten and fourteen layers respectively. In this case the single fiber collection efficiency of the first and second layers and the corresponding values of m can be evaluated directly. To obtain the relevant quantities for a filter with four layers, $(E_t)_3$ was assumed to be the arithmetic average of $(E_t)_2$ and $(E_t)_4$. This estimated $(E_t)_3$ was then used to calculate η_4 . The corresponding value of m was obtained by assuming that the extent of deposition on the third and fourth layers of screen was the same. The same principle was used to calculate the values of η_6 (and the corresponding values of m_6) and applied to data obtained with 200 mesh and 500 mesh screens as well.

The sequence of steps in developing a correlation between the single fiber efficiency, η , and the amount of deposition, m is as follows. The experimentally determined total collection efficiency, E_t , for model filters with different layers of 500 mesh screens at one velocity ($V_{\infty} = 14.5$ cm/s) and those obtained with model filters with a single 500 mesh screen but at different gas velocities are plotted as functions of $C_{in} V_{\infty} \theta$ (Figures 12 and 13). With the use of Eqs. 19 and 21 and the procedure outlined before, the value of η at various m were calculated. For data obtained from model filters composed of various layers of the same kind of screen at the same velocity, η is found to be a linear function of m and exhibits dependence on the number of screen layers (as shown in Figure 14). However, the results obtained using the single layer of screen show a strong dependence on gas velocity. Even when the data are plotted in the form of η/η_0 vs. m there is still considerable scattering. However, by trial and error, it was possible to express all the collection efficiency data (obtained with different sizes of screens and at different gas velocities) by the expression

$$\frac{\eta}{\eta_0} = 1 + \left(\frac{m}{m_0}\right)^b \quad (22)$$

where η_0 is the initial collection efficiency and m_0 is the value of m at which the increase in η over η_0 is 100%. [Note that by this definition, the curve $(\eta/\eta_0 - 1)$ vs. m/m_0 passes through the point

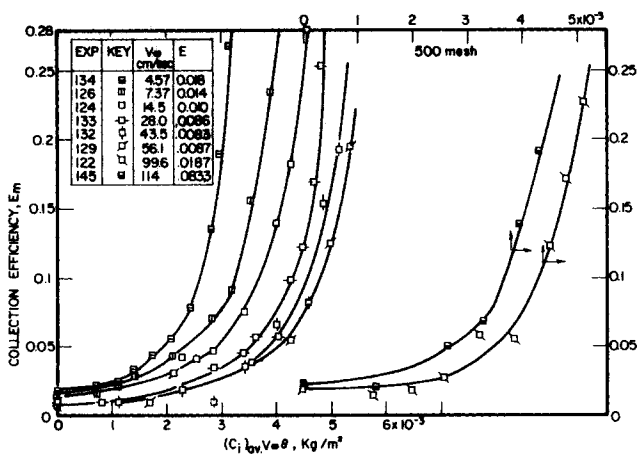


Figure 13. Collection efficiency of single layer model filter at different gas velocities.

(1, 1)]. This is shown in Fig. 15 for the data obtained with the use of 200 mesh screens.

The empirical exponent, b , is found to be

Screen Size	b
200 mesh	1.15
325 mesh	1.23
500 mesh	1.34

The clean single fiber efficiency, η_o , can be obtained from Figure 9 or, in principle, from the classical trajectory calculation based on the parallel fiber model (Tsiang, 1980). On the other hand, the critical mass deposit, m_o , is a quantity which varies with the dimension of the screen, gas velocity, V_∞ and the type of screen as shown in Figure 16. The results can be approximated by the following empirical expression

$$m_o = A \eta_o V_\infty^{0.25} \quad (23)$$

where $A = 2.7 \times 10^{-3}$, 1.5×10^{-3} and 1.1×10^{-3} for the 200, 325 and 500 mesh screens respectively. V_∞ is given in cm/s and m_o in kg/m².

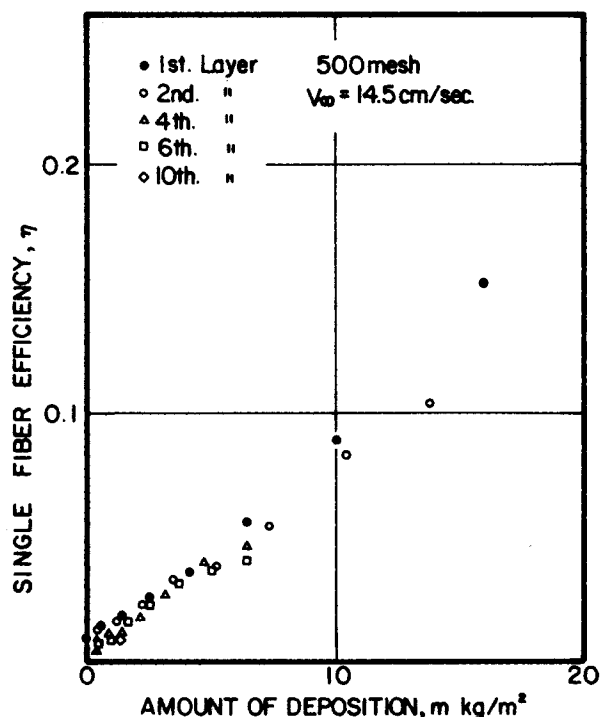


Figure 14. Single fiber efficiency vs. amount of deposition at one gas velocity.

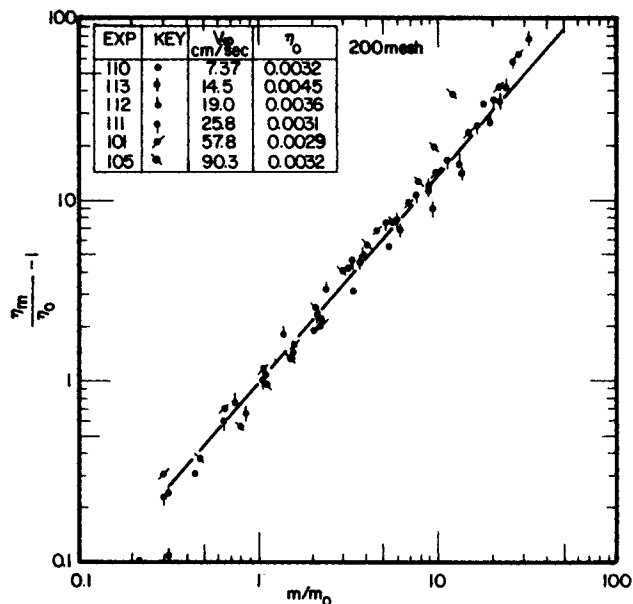


Figure 15. $\left(\frac{\eta}{\eta_o} - 1\right)$ vs. $\left(m/m_o\right)$.

The correlations presented above are valid only under conditions similar to those used to obtain the model filter data, i.e., the three types of wire screens and aerosol particles of 1.1 μm in diameter. Applications of the correlations to conditions significantly different from those used in the experimental work would likely lead to error. On the other hand, the fairly good correlations obtained in the study suggest that the format of the correlation expressions established in this work should be applicable to model filters composed of wire screens in general. It would be necessary to establish proceedings which can be used to predict b and m_o/η_o . This however cannot be attempted without additional data.

Attempts were also made to develop correlations for the pressure drop increase across a single screen layer as a function of the mass of deposit as well as the pertinent system and operating variables. This, however, was unsuccessful. The increase in pressure drop, expressed as $(\Delta p/\Delta p_o) - 1$ where Δp and Δp_o are the pressure drop across a single screen layer and the pressure drop across a single clean screen layer respectively is indeed a function of m as shown in Figure 17. It was not possible to relate the pressure drop increase, $[(\Delta p)/\Delta p_o] - 1$ with the amount of deposit particles in a systematic manner.

In the absence of any other alternatives, the relative pressure drop increase data were correlated with the mass of deposit, m , irrespective of the gas velocities used in the measurements. For the 200 mesh screen data, the result is found to be

$$\left(\frac{\Delta p}{\Delta p_o} - 1\right) = (1.997 \times 10^{10}) m^{2.73} \quad (24)$$

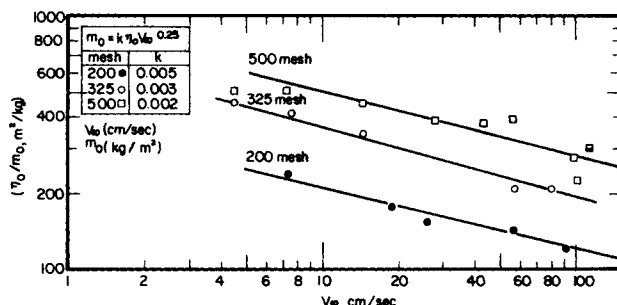


Figure 16. Relationship between m_o and V_∞ .

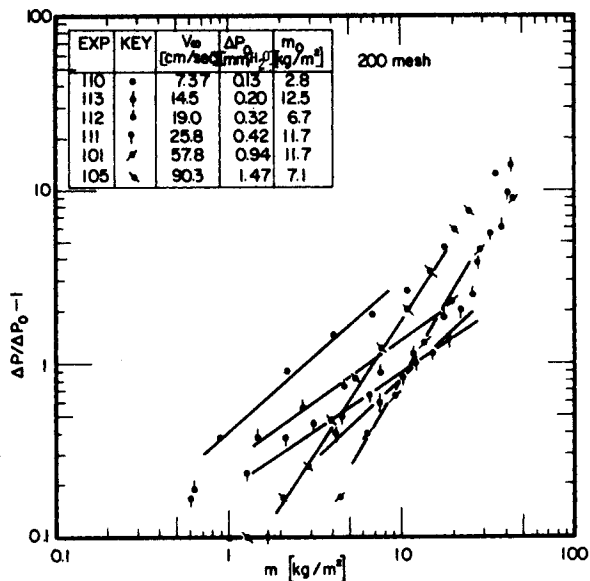


Figure 17. Pressure drop increase vs. m (200 mesh).

Similar expressions were obtained for the 325 mesh and 500 mesh data. The coefficients are 8.440×10^9 and 1.275×10^7 and the exponents are 2.579 and 1.689 for the 325 mesh and 500 mesh cases respectively. It should be emphasized that these expressions are very approximate and should be used for the order of magnitude estimate of pressure drop increase.

STIMULATION OF THE DYNAMIC BEHAVIOR OF MODEL FIBROUS FILTERS

The twin features of the dynamic behavior of a filter bed are the history of the effluent concentration and that of the pressure drop across the bed. The results of the present work make it possible to

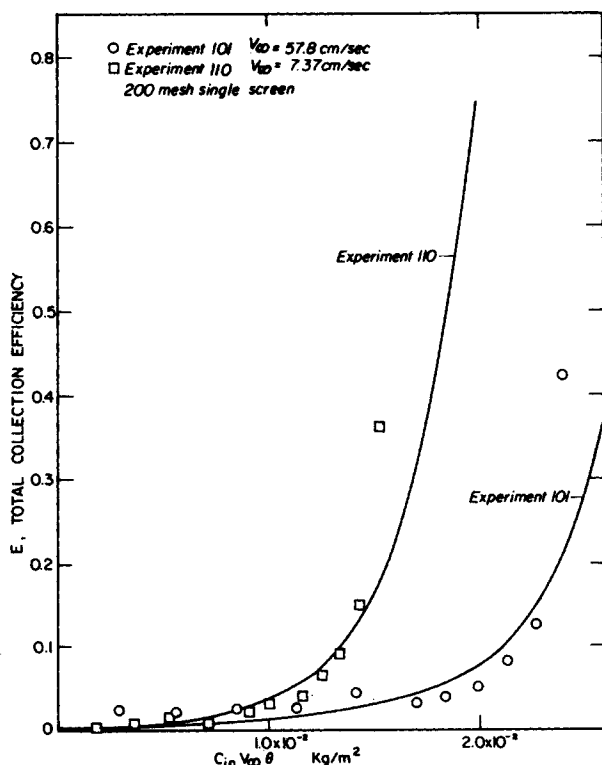


Figure 18. Predictions of single screen model filter performance based on empirical correlations developed in this work and their comparison with data.

predict such behavior of model filters composed of layers of wire screens. From Eq. 17 one has

$$\frac{C_k}{C_{k-1}} = \left[1 - \frac{a_c}{h} \eta_k \right]^2 \quad (27)$$

$$\text{for } k = 1, 2, \dots$$

$$\eta_k = \eta_0 \text{ at } \theta = 0 \quad (26)$$

Also, rewrite Eq. 21 as follows

$$m_k = V_{\infty} \int_0^{\theta} (C_{k-1} - C_k) d\theta \quad (26)$$

Equations 17, 25 and 26, together with the correlations of η vs. m (Eq. 22), can be used to obtain the effluent concentrations ($C_{\text{eff}} = C_n$) as a function of time in an incremental and iterative way. First, by letting $k = 1$ for Eq. 17 and assuming that $\eta_1 = \eta_0$, (η_0 , the initial single fiber efficiency is assumed to be known), an estimate of c_1 can be obtained. This information, together with Eq. 26, provides an estimation of the amount of deposit of the first screen layer, m_1 as a function of time; which can be used to estimate the value of η_1 as a function of time with the use of Eq. 22. This new estimate of η_1 can then be used to obtain a second approximation of m_1 . This iteration can be continued until the desired accuracy is reached. Once c_1 and m_1 are known as functions of θ , the values of c_2 and m_2 can be found from the procedure as outlined before. These procedures can be extended to the last screen layer to obtain the effluent particle concentration history. Further, with m_1, m_2, \dots, m_n known, a rough estimate of pressure drop across each layer can be found from Eqs. 24 to 26, the sum of which yields the history of the total pressure drop across the model filter. The results of some sample calculations and their comparisons with experimental data are shown in Figure 18.

ACKNOWLEDGMENT

The study was performed under a contract from the Empire State Electrical Energy Research Corporation (Contract No. EP 8-4).

NOTATION

- A = coefficient of Eq. 23
- a_o = constant defined by Eq. 12
- a_c = radius of wire
- a_p = radius of aerosol particle
- b = empirical exponent of Eq. 22
- C_D = drag coefficient
- C_s = Cunningham correction factor
- C_{in} = particle concentration of influent
- C_{eff} = particle concentration of effluent
- C_k = particle concentration of gas leaving the k -th screen layer
- d_p = diameter of particle
- E_k = collection efficiency of the k -th screen layer
- E_o = initial total collection efficiency
- $(Et)_n$ = total collection efficiency of a model filter composed of n layers of screen
- F_D = drag force acting on a single clean wire
- h = half-distance between two adjacent wires of a screen
- m_k = mass deposit of the k -th layer screen
- m_o = critical mass deposit
- N_R = relative size parameter, defined as a_p/a_c
- N_{Re} = Reynolds number defined as $\rho V_{\infty}(2a_c)/\mu$
- N_{St} = Stokes number defined as $2 C_s \rho_p a_p^2 V_i/9\mu a_c$
- t = quantity defined by Eq. 13
- V_{∞} = superficial velocity of gas
- W^* = clearance between two adjacent wires

Greek Letters

Δp	= pressure drop across a screen layer
Δp_o	= pressure drop across a clean screen layer
ρ	= density of gas
ρ_p	= density of particle
η_o	= initial single fiber efficiency
η_k	= single fiber efficiency for the k -th layer screen
θ	= time
μ	= gas viscosity

LITERATURE CITED

- Davies, C. N., "Air Filtration," Academic Press (1973).
Dymont, J., "Theory and Practice in Air Filtration," *Depositton and Filtration of Particles from Gases and Liquids*, p. 183, Soc. Chem. Ind., London (1978).
First, M. W. and W. C. Hinds, "High Velocity Filtration of Submicron Aerosols," *J. Air Poll. Control Assoc.*, **26**, 119 (1976).

- Fuchs, N. A. and I. B. Stechkina, "A Note on the Theory of Fibrous Aerosol Filters," *Ann. Occup. Hyg.*, **6**, 27 (1963).
Gentry, J. M. and K. R. Choudhary, "Collection Efficiency and Pressure Drop in Grid Filters of High Packing Density at Intermediate Reynolds Numbers," *J. Aerosol Sci.*, **6**, 277 (1975).
Liu, Y. H., K. T. Whitby, and H. Yu, "A Condensation Aerosol Generator for Producing Monodispersed Particles in the Size Range of 0.036 μ m to 1.3 μ m," *J. de Res. Atm.*, **3**, 397 (1966).
Miyagi, T., "Viscous Flow at Low Reynolds Numbers Past an Indefinite Row of Equal Circular Cylinders," *J. Phys. Soc., Japan*, **13**, 493 (1958).
Muir, D. C. F. and C. N. Davies, "The Deposition of 0.5 μ Diameter Aerosols in the Lungs," *Ann. Occup. Hyg.*, **10**, 161 (1967).
Tsiang, R. C. C., "Mechanics of Particle Deposition on Model Filters Composed of an Array of Parallel Fibers," Ph.D. Dissertation, Syracuse University, Syracuse, NY (1980).
Whipple, R. T., "The Dispersion of Aerosols in a Model of Human Upper Respiratory Tract," M.S. Thesis, Syracuse University, Syracuse, NY (1972).

Manuscript received October 8, 1980, revision received June 15, and accepted July 14, 1981.

Heterogeneous Catalytic Reactors Undergoing Chemical Deactivation

Part I: Deactivation Kinetics and Pellet Effectiveness

A general expression for the time-dependence of the activity of a catalyst pellet affected by both chemical deactivation and diffusion is developed. Specific results are given for both uniform and pore-mouth poisoning, with parallel and series poisoning mechanisms. Comparisons show a satisfactory agreement between theoretical and experimental results. A pellet effectiveness representing the combined effect of deactivation and diffusion is also developed in a form suitable for direct inclusion in reactor conservation equations.

H. H. LEE

Department of Chemical Engineering
University of Florida
Gainesville, FL 32611

J. B. BUTT

Department of Chemical Engineering
and
Ipatieff Catalytic Laboratory
Northwestern University
Evanston, IL 60201

SCOPE

The time dependence of loss of catalytic activity due to various mechanisms of deactivation is often described by empirical correlations based on time-on-stream. A few specific results of more theoretical nature are available and have been described by Carberry (1976), but these are very limited. An ultimate goal would be to describe the observable time dependence of the main and deactivation reactions in terms of pertinent physical

and chemical parameters that can be determined in independent experimentation. In the present work we propose a formulation, so based, for description of the time dependence of loss of catalytic activity. The approach considers both deactivation and diffusion limitation in individual particles and yields a pellet effectiveness that can be incorporated directly into reactor design models.

CONCLUSIONS AND SIGNIFICANCE

A mechanistic representation of chemical deactivation by parallel and sequential schemes leads to a general form of deactivation kinetics that gives relatively simple expressions for pellet effectiveness for both uniform and pore-mouth poisoning. The agreement between theory and experimental data

obtained for parallel pore-mouth poisoning is satisfactory, although it is shown that intraparticle diffusivity is a sensitive parameter. The quantities appearing in the theory are all accessible to determination in separate experimentation. Finally, the pellet effectiveness, expressed in terms of pellet surface conditions, is simple enough to be directly incorporated into reactor conservation equations, allowing some simplification of an inherently complicated design problem.